Association between different levels of lipid metabolism-related enzymes and fatty acid synthase in Wilms' tumor

XIAOQING WANG[1*], GUOQIANG DU[1*], YIDI WU[1],
YONGFEI ZHANG[2], FENG GUO[1], WEI LIU[1] and RONGDE WU[1]

[1]Department of Pediatric Surgery, Shandong Provincial Hospital Affiliated to Shandong University, Jinan, Shandong 250021; [2]Department of Dermatology, Shandong Provincial Qianfoshan Hospital Affiliated to Shandong University, Jinan, Shandong 250014, P.R. China

Received August 17, 2019; Accepted December 6, 2019

DOI: 10.3892/ijo.2019.4948

Abstract. Wilms' tumor is one of the most common malignant tumors of the abdomen in children. However, there is currently no recognized specific biomarker for the clinical diagnosis and prognosis of this tumor. Lipid metabolism is involved in membrane synthesis and oxidation in tumor cells. This process plays an important role in the development of tumors, but it has not yet been investigated in Wilms' tumor. The aim of the present study was to characterize the changes in lipid metabolism and to contribute to the diagnosis and prognosis of Wilms' tumor. Proteomics analysis was performed to detect lipid-metabolizing enzymes in 9 tissue samples from Wilms' tumors and adjacent tissues, and proteomics revealed the presence of 19 differentially expressed lipid-metabolizing enzymes. Protein interaction analysis with the Search Tool for the Retrieval of Interacting Genes/Proteins was used to identify the interacting proteins. Immunohistochemistry (IHC), immunofluorescence and western blotting were used to further confirm whether the expression of fatty acid synthase (FASN) was significantly increased in the tumor tissues. Oncomine database and reverse transcription-PCR analyses further confirmed that the expression of FASN at the gene level was significantly increased in the tumors. Following collection of 65 pediatric cases of Wilms' tumor at the Shandong Provincial Hospital between 2007 and 2012, the association between the expression of FASN and the clinical characteristics was analyzed, and IHC analysis further demonstrated that FASN expression was significantly associated with tumor stage and size. The association between FASN and the prognosis of children with Wilms' tumor was analyzed using Kaplan-Meier survival curves. In addition, univariate survival analysis revealed that higher expression of FASN in Wilms' tumors was associated with poorer prognosis. Our findings revealed that FASN may be used as a prognostic biomarker in patients with Wilms' tumor. Furthermore, lipid metabolism may play an important role in the occurrence and development of Wilms' tumor.

Correspondence to: Dr Rongde Wu or Dr Wei Liu, Department of Pediatric Surgery, Shandong Provincial Hospital Affiliated to Shandong University, 324 Jingwu Street, Jinan, Shandong 250021, P.R. China
E-mail: wrd2190@163.com
E-mail: lemontree1119@126.com

*Contributed equally

Key words: Wilms' tumor, lipid metabolism, fatty acid synthase, mass spectrometry, prognosis

Introduction

Wilms' tumor is one of the most common malignant tumors of the abdomen in children. The prognosis of this cancer is associated with age, tumor size and histological type. However, the most important prognostic factor is local invasion and distant metastasis of the tumor (1). The mechanism underlying the pathogenesis and metastasis of Wilms' tumor have yet to be fully elucidated, and further research is required to design targeted therapies.

The role of lipid metabolism in cancer is attracting increasing attention, and inhibition of lipid autophagy has been shown to be of clinical value in other tumors (2). Due to the high metabolic demands of tumor cells and their nutritional deficiency during chemoradiotherapy, fatty acid metabolism can provide the necessary energy for tumor cells. Furthermore, tumor cell division requires a high energy supply. As phospholipids are an important part of the cytoskeleton, phospholipid synthesis provides essential raw materials for tumor cell proliferation (3-5). Thus, recent publications have reported that lipid metabolism is closely associated with tumor cell proliferation, invasion, migration and chemosensitivity (6,7), and it is emerging as an attractive target for cancer drug discovery.

Fatty acid synthase (FASN) is essential for *de novo* lipogenesis and cellular substrate energy metabolism, including the synthesis of long-chain fatty acids from acetyl-CoA, malonyl-CoA and NADPH (8,9). The expression of FASN also has a considerable impact on tumor progression: The expression of FASN in a variety of solid tumors was found to be significantly increased and was associated with poor prognosis (10), and the proliferation, invasion and migration of

tumor cells were significantly suppressed after its downregulation (11-13). In particular, in renal cell carcinoma, Albiges *et al* demonstrated that FASN played an important role in the occurrence of tumors and that patients with higher expression levels had a poor prognosis (14). However, only few studies (15) have addressed the role of FASN in Wilms' tumor.

Investigating the effect and mechanism of action of FASN, a lipid-metabolizing protein, on the metastasis of Wilms' tumors may provide a novel approach to the targeted therapy of this disease. The aim of the present study was to examine the different levels of lipid metabolism-related enzymes and determine whether FASN is a key factor in the progression of Wilms' tumor.

Materials and methods

Tissues. Between January 2007 and January 2012, a total of 65 patients with Wilms' tumor who did not undergo radical or palliative nephrectomy were selected for immunohistochemistry (IHC) analysis. Clinical data, including sex, age, tumor size, stage, histopathological type, metastasis and follow-up information, were recorded. The patients included 35 males and 30 females, with a mean age at diagnosis of 3.2 years (range, 0.25-11.8 years). Detailed information may be found in Table I. The duration of the follow-up was 60 months. In addition, 20 cases of Wilms' tumor and adjacent tissues collected between March 2015 and December 2017 and stored at -80˚C were selected. The tumors were graded according to the Fuhrman nuclear grade classification (16) as follows: G1, n=10; G2, n=7; and G3, n=3. A total of 9 cases (G1, n=3; G2, n=3; and G3, n=3) were used for label-free quantification. Radiotherapy, chemotherapy and immunotherapy were not performed prior to surgery, and the samples were verified by two pathologists postoperatively. The study protocol was approved by the Ethics Committee of Shandong Provincial Hospital Affiliated to Shandong University, and the legal guardians of the patients provided informed consent regarding the use of the patients' tissues for research purposes.

Protein digestion. Proteins were re-dissolved in 500 mM triethylammonium bicarbonate (TEAB). The protein concentration of the supernatant was determined using the BCA protein assay, and 100 μg protein per condition was transferred into a new tube and adjusted to a final volume of 100 μl with 8 M urea. Subsequently, 11 μl of 1 M DTT was added, and the sample was incubated at 37˚C for 1 h and transferred into a 10 K ultrafiltration tube (EMD Millipore). To remove the urea, the samples were centrifuged after adding 100 mM TEAB three times at 14,000 x g at 4˚C for 10 min, followed by the addition of 120 μl of 55 mM iodoacetamide to the sample and incubation for 20 min in the dark at room temperature. The proteins were then digested with sequencing grade modified trypsin (Promega Corporation).

Label-free quantification. First, 18 cases of in-solution digestion samples (Wilms' tumor and their adjacent tissues; G1, n=3; G2, n=3; and G3, n=3) were acquired and analyzed by nanoflow liquid chromatography-tandem mass spectrometry (nanoLC-MS/MS). The samples were resuspended in 30 μl solvent C (C: water with 0.1% formic acid; D: ACN with 0.1% formic acid), separated by nanoLC and analyzed by online electrospray MS/MS. The experiments were performed on an Easy-nLC 1000 system (Thermo Fisher Scientific, Inc.) connected to a Q-Exactive mass spectrometer (Thermo Fisher Scientific, Inc.) equipped with an online nano-electrospray ion source. A 10-μl peptide sample was loaded onto the trap column (Acclaim PepMap C18, 100 μm x 2 cm, Thermo Fisher Scientific, Inc.) at a flow rate of 10 μl/min for 3 min, and subsequently separated on the analytical column (Acclaim PepMap C18, 75 μm x 15 cm) with a linear gradient from 3% D to 32% D in 60 min. The column was re-equilibrated at the initial conditions for 10 min. The column flow rate was maintained at 300 nl/min. The electrospray voltage of 2 kV vs. the inlet of the mass spectrometer was used.

The mass spectrometer was run under data-dependent acquisition mode and automatically switched under MS and MS/MS mode. The MS1 mass resolution was set as 35 K with m/z 350-1,550, and the MS/MS resolution was set as 17.5 K under HCD mode. The dynamic exclusion time was set at 20 sec.

Volcano plot. The volcano plot, which plots significance vs. fold-change on the y and x axes, respectively, is a type of scatter plot that is used to quickly identify changes in large datasets composed of replicate data. This plot is drawn by using the ggplot2 package (http://ggplot2.org).

Hierarchical cluster analysis (HCA). HCA is an algorithmic approach to finding discrete groups with varying degrees of (dis)similarity in a dataset represented by a (dis)similarity matrix. This analysis is processed with the pheatmap package (https://CRAN.R-project.org/ package=pheatmap).

Gene Ontology (GO) analysis. Blast2GO version 4 (BioBam Bioinformatics S.L.) was used for functional annotation. The whole protein sequence database was analyzed by BlastP using a whole database and mapped and annotated with a GO database. Statistically altered functions of differentially expressed proteins were calculated by Fisher's exact test in Blast2GO.

Search Tool for the Retrieval of Interacting Genes/Proteins (STRING) analysis. The protein-protein interaction network was analyzed using STRING v.10 (http://string-db.org/).

Database for Annotation, Visualization and Integrated Discovery (DAVID) functional annotation tool. The differentially expressed proteins were also identified using DAVID functional annotation for functional analysis (https://david.ncifcrf.gov/).

Kyoto Encyclopedia of Genes and Genomes (KEGG) analysis. Pathway analysis was processed by KOBAS (http://kobas.cbi.pku.edu.cn/). Pathways with $P<0.05$ were recognized as significantly altered.

Ingenuity Pathway Analysis (IPA). IPA is a common tool used to model, analyze and understand complex biological systems, particularly to reveal different signaling networks and biological processes (17). IPA is an integrated biological pathway analysis software based on cloud computing. With

Table I. Correlation of expression levels of the FASN protein with the clinicopathological parameters of patients with Wilms' tumor.

Clinicopathological parameters	n (%)	FASN expression		P-value
		High	Low	
Sex				0.620
Male	35 (53.8)	17	18	
Female	30 (46.2)	17	13	
Age (months)				0.083
>24	28 (43.1)	11	17	
≤24	37 (52.9)	23	14	
Stage				
I	32 (49.2)	9	23	
II	21 (32.3)	16	5	0.001 (II vs. I)
III	12 (18.5)	9	3	0.007 (III vs. I)
Histopathological type				0.032
Favorable	46 (70.8)	20	26	
Unfavorable	19 (29.2)	14	5	
Lymphatic metastasis				0.086
Yes	10 (15.4)	8	2	
No	55 (84.6)	26	29	

FASN, fatty acid synthase.

the support of the highly structured bioinformatics platform Ingenuity Knowledge Base, it can search for various types of related information on genes, proteins and drugs, as well as constructing interaction models. In addition, this tool can also analyze data obtained through such techniques as genomics, microRNA, experimental data for single-nucleotide polymorphisms, chips, metabolomes and proteomes.

Immunohistochemistry analysis. Tissues obtained from Wilms' tumors were subjected to fixation with 4% paraformaldehyde for at least 72 h at room temperature, dehydration using 10% formalin for 3 h, followed by immersion in a series of graded ethanol baths, washing in xylene, immersion and final embedding in paraffin. The tissue blocks were cut into 5-μm sections. After dewaxing and rehydration, heat-induced epitope retrieval was performed with 1 mM EDTA (pH 9.0) in a microwave oven. Then, samples were immersed in 3% H_2O_2 aqueous solution for 30 min to exhaust endogenous peroxidase. After closure blocking with goat serum for 30 min, the sections were incubated overnight at 4˚C with primary anti-FASN antibody (dilution 1:100, cat. no. 10624-2-AP, ProteinTech Group, Inc.). Peroxidase-labeled secondary antibodies were applied, and diaminobenzidine (DAB; Zhongshan) staining was performed at 4˚C for 10 sec. The slides were then counterstained with hematoxylin at room temperature for 4 min and mounted. As a negative control, samples were analyzed without the primary antibody.

Western blot analysis. To determine the FASN level, proteins were extracted from the tissues by suspension in radioimmunoprecipitation assay (RIPA) buffer (Solarbio). The samples were centrifuged at 13,523 x g at 4˚C for 38 min, and the supernatants were recovered for analysis. The protein concentration was determined using the bicinchoninic acid (BCA) protein assay kit (Sigma-Aldrich; Merck KGaA). Protein samples (40 μg) were electrophoresed on a pre-cast bis-Tris polyacrylamide gel (8-12%) and then transferred onto a polyvinylidene difluoride membrane (EMD Millipore). The membranes were blotted with rabbit anti-FASN (1:1,000) and mouse anti-actin (all from ProteinTech Group, Inc.) followed by horseradish peroxidase (HRP)-conjugated secondary antibodies (1:5,000; ZsBio). Immunoblots were visualized using enhanced chemiluminescence (LAS-4000; GE Healthcare).

mRNA expression analysis. The expression of the FASN gene was analyzed by RT-qPCR. RNA was isolated from 40 frozen samples (20 from Wilms' tumors and 20 from adjacent tissues) from which sufficient material was obtained with the miRVana miRNA Isolation Kit (TaKaRa Bio, Inc.). The quantity and quality of total RNA was determined with a Nanodrop ND-2000 Spectrophotometer (Thermo Fisher Scientific, Inc.). RT (37˚C 15 min, 85˚C 5 sec, and held at 4˚C until use) was performed using the TaqMan Reverse Transcription kit (Applied Biosystems; Thermo Fisher Scientific, Inc.) in the GeneAmp PCR 9700 system and RT-qPCR amplification with the TaqMan Universal PCR Master Mix (Applied Biosystems; Thermo Fisher Scientific, Inc.). All RT-qPCR measurements were obtained in a 7900HT Fast Real Time PCR System with the ExpressionSuite Software v1.0 (Applied Biosystems; Thermo Fisher Scientific, Inc.). All siRNAs were purchased from Personalbio, and their sequences were as follows: 5'-CTC ATCAAGTGGGACCACAG-3' (forward) and 5'-CAGCGT CTTCCACACTATGC-3' (reverse) for FASN; 5'-AATCGT GCGTGACATTAAGG-3' (forward) and 5'-TAGTTTCGT

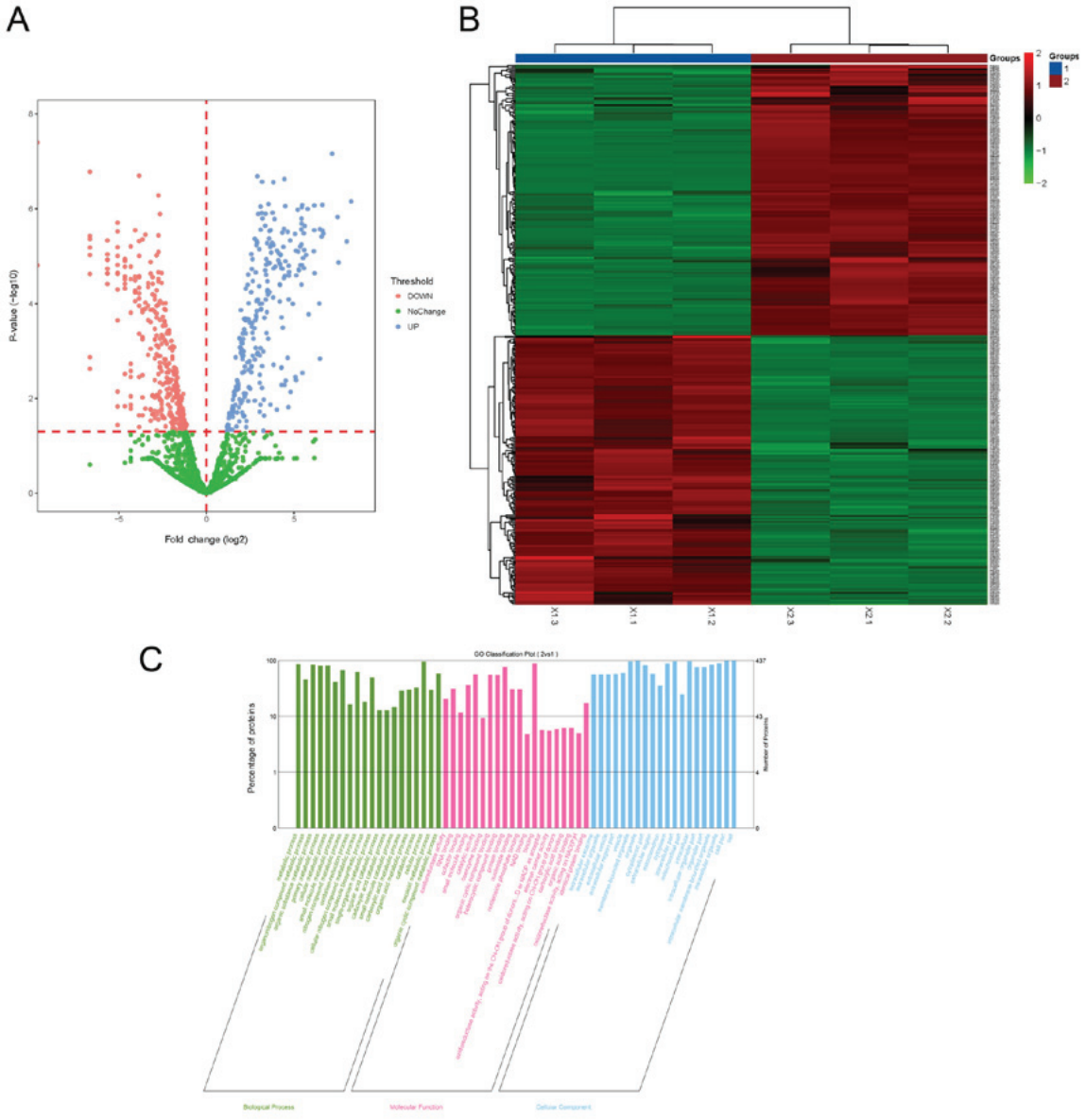

Figure 1. Label-free quantification and analysis. (A) The volcano plot is a scatter plot with the log2 value of the fold change as the horizontal axis and the -log10 change of the P-value as the vertical axis. The data are mainly divided into three major points according to the threshold of the significant change. Red dot, upregulation (219 proteins); blue dot, downregulation (218 proteins); and green dot, unchanged (Wilms' tumor vs. adjacent tissues). (B) The heat map, also referred to as hierarchical cluster analysis, indicates the extent of the peptide or protein expression in terms of the depth of color. In the vertical axis the sample is clustered, and the peptide is aligned in the horizontal axis. Segment or protein for cluster analysis. (C) Gene Ontology (GO) classification results are visualized using bar graphs. The GO classification bar graph uses the top 20 pathways with the smallest P-value. The ordinate indicates the number of proteins in each secondary classification and their percentage of the total number of differential proteins. The color indicates different primary classifications. Biological process (green), molecular function (red); and cellular component (blue). As marked in the figure, Group 1 indicates tumor tissue and Group 2 adjacent tissue.

GGATGCCACAG-3' (reverse) for actin. RT-qPCR analysis was performed using SYBR Premix Ex Taq™ II (Takara, Japan), according to the manufacturer's protocol. The qPCR reactions were performed on a Roche 480 Real-Time PCR System using the standard procedure for two-step PCR amplification as follows: Pre-denaturation at 95˚C for 30 sec, PCR at 95˚C for 5 sec, 60˚C for 30 sec, for 40 cycles; melting curve: 95˚C for 5 sec, 60˚C for 60 sec, 95˚C for 15 sec; cooling: 50˚C for 30 sec. After the reaction, the amplification curve and melting curve of qPCR were confirmed and data were analyzed (18). The FASN mRNA expression levels were examined using the $2^{-\Delta\Delta Cq}$ method and were compared against the level of actin (19).

Immunofluorescence. Cell concentration smears were performed and the cells were fixed with 4% paraformaldehyde at room temperature for 20 min. The cells were thoroughly rinsed with 0.01 M PBS (5 min x 3) and incubated in 0.3% Triton at room temperature for 20 min, followed by washing in 0.01 M PBS (5 min x 3). Next, 30 μl/sample goat serum blocking solution was added at room temperature for 60 min followed by primary antibody at 30 μl/sample (1:100 diluted in goat serum). The cells were placed in a wet box at 4˚C overnight and then washed in 0.01 M PBS (5 min x 3). On the next day, fluorescent secondary antibody (dilution 1:100) was added at 30 μl/sample (10% skimmed milk powder) at room temperature in the dark for 60 min, followed by addition

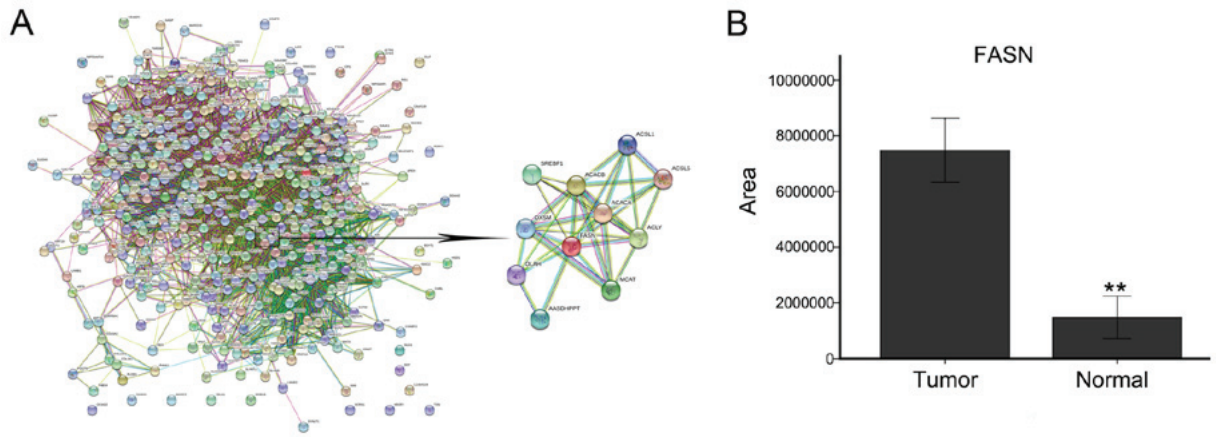

Figure 2. Mass spectrometry shows the interactions of the 437 proteins and the expression level of FASN. (A) Visualization of protein-protein interactions among the dysregulated proteins in Wilms' tumors using STRING analysis (confidence mode). There was an association among 418 proteins. A total of 437 proteins were input into the STRING software. The lines represent interactions between proteins. (B) Mass spectrometry demonstrated the expression of FASN. FASN expression was found to be upregulated in tumor tissues (**P<0.01 vs. adjacent tissue). Data are expressed as the mean ± standard deviation of 3 independent experiments. FASN, fatty acid synthase; STRING, Search Tool for the Retrieval of Interacting Genes/Proteins.

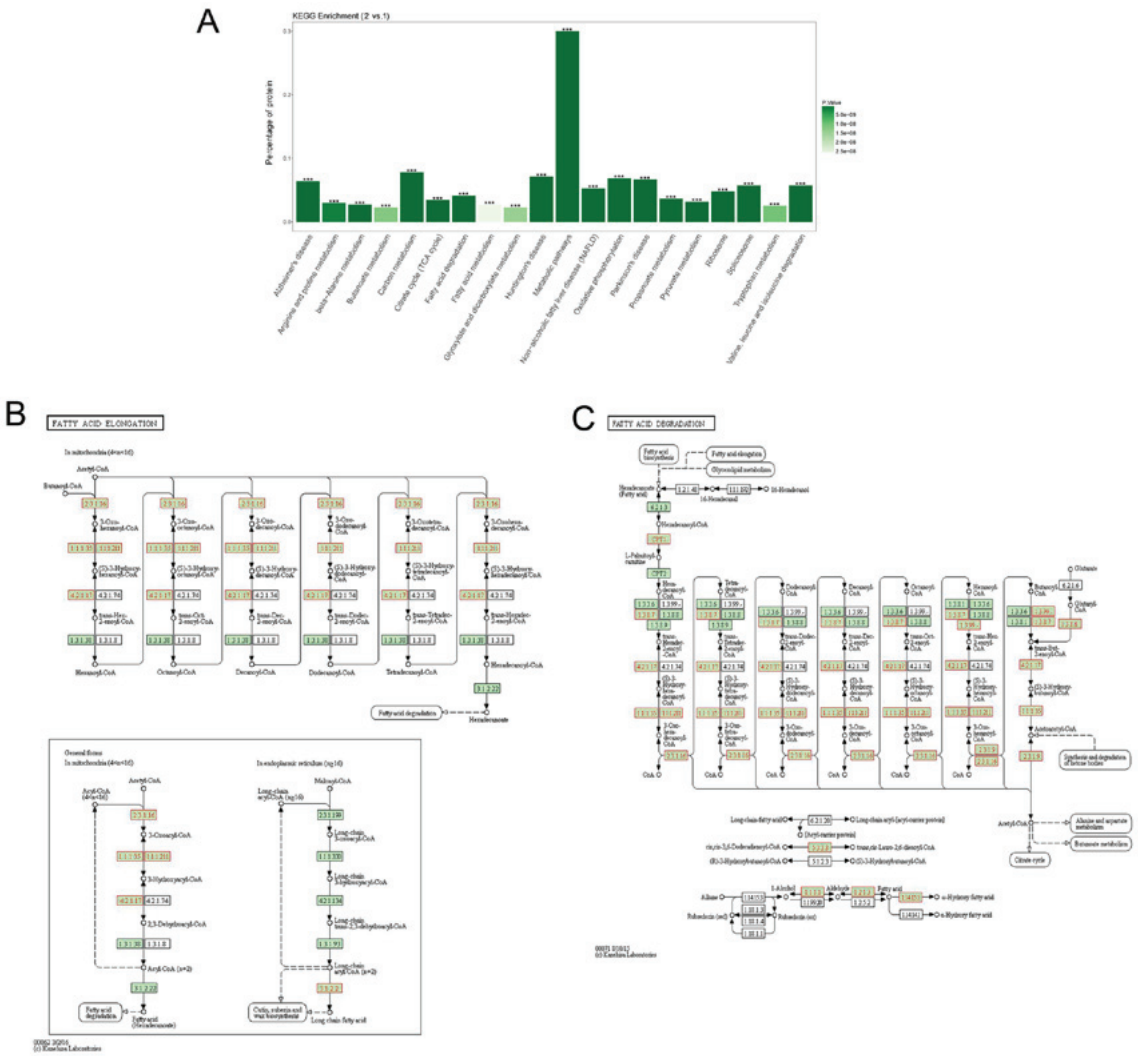

Figure 3. KEGG analysis of the 437 differentially expressed proteins. (A) The KEGG enrichment results can be visualized by bar graphs, and the top 20 pathways with the smallest P-value are plotted. The ordinate indicates the percentage of total protein in the pathway. The darker the color, the smaller the P-value. ***P<0.001. (B) The selected enzymes are involved in the process of long-chain fatty acid extension. (C) The selected enzymes are involved in the process of fatty acid degradation. The EC code is concluded, such as ACAA [EC:2.3.1.16], ECHS1 [EC:4.2.1.17], ACSF2 [EC:6.2.1.2], EHHADH [EC:4.2.1.17&1.1.1.35&5.3.3.8], ACADM [EC:1.3.8.7], ACADSB [EC:1.3.99.12], ECH1 [EC:5.3.3.21], DECR1 [EC:1.3.1.34], HADHA [EC:4.2.1.17&1.1.1.211] (https://www.kegg.jp/). Group 1, tumor tissue; Group 2, adjacent tissue. (B and C) Green node, species-specific; blue frame node, downregulation; and red frame node, upregulation. KEGG, Kyoto Encyclopedia of Genes and Genomes.

of 4',6-diamidino-2-phenylindole (DAPI) for 10 min. Next, the cells were washed in 0.01 M PBS (5 min x 3) and mounted with an anti-fluorescence quencher.

Statistical analysis. The data were statistically analyzed using Student's t-test, the χ^2 test, or Fisher's exact test using SPSS version 19.0 (SPSS, Inc.). The survival curves were analyzed by the Kaplan-Meier method. P<0.05 was considered to indicate statistically significant differences. Tandem mass spectra were processed by PEAKS Studio version 8.0 (Bioinformatics Solutions, Inc.). Differentially expressed proteins were filtered if their fold change was >2 and their P-value was <0.01 (significant >20). The P-value for IPA data analysis was based on the Right-Tailed Fisher's Exact Test algorithm.

Results

MS revealed 19 differentially expressed lipid metabolism-related enzymes in tumors and adjacent tissues. Label-free proteomics analysis revealed that there were 219 upregulated and 218 downregulated proteins in the tumor (Fig. 1). The HCA map indicates the extent of the peptide or protein expression in terms of depth of color, and the GO classification results can be visualized using bar graphs. The GO classification bar graph uses the top 20 pathways with the smallest P-value (Fig. 1). The results were divided into biological processes, molecular functions and cellular components. As shown in Fig. 2, 437 proteins were input into STRING software, and there were associations among 418 of those proteins. Subsequently, the DAVID functional annotation tool was used to perform protein functional analysis. Among the 437 proteins, 19 were associated with lipid metabolism, including lipid synthesis and decomposition (Fig. 3B). The upregulated proteins included FASN, inositol-3-phosphate synthase 1 (ISYNA1), and arachidonate-15-lipoxygenase (ALOX15), and the downregulated proteins included hydroxyacyl coenzyme A dehydrogenase beta [HADHB (Fig. 3C)], acetyl coenzyme A acyltransferase 1 (ACAA1), acetyl coenzyme A acyltransferase 2 (ACAA2), carnitine palmitoyltransferase 1A (CPT1A), enoyl-coenzyme A hydratase (ECHS1), acyl-CoA synthetase family member 2 (ACSF2), enoyl-coenzyme A, hydratase/3-hydroxyacyl coenzyme A dehydrogenase (EHHADH), pyruvate carboxylase (PC), acyl-CoA dehydrogenase medium-chain (ACADM), short/branched chain acyl-CoA dehydrogenase (ACADSB), enoyl coenzyme A hydratase 1 (ECH1), GM2 ganglioside activator (GM2A), 2,4-dienoyl-CoA reductase 1 (DECR1), hydroxyacyl coenzyme A dehydrogenase alpha [HADHA (Fig. 3C)], ubiquinone oxidoreductase subunit AB1 (NDUFAB1) and histone H3.3 [H3F3A (Fig. 4)].

KEGG pathway analyses for lipid metabolism. Fatty acid, triacylglycerol and ketone body metabolism pathway analysis uncovered lipid metabolism-related proteins or protein complexes, small molecules, and their interactions (Fig. 3). KEGG enrichment provides plotting of the top 20 pathways with the smallest P-value. The ordinate indicates the percentage of total protein in the pathway. Fatty acid metabolism and fatty acid degradation are included among the top 20 most highly expressed signaling pathways. The KEGG signaling pathway demonstrated the pathways of fatty acid elongation and fatty

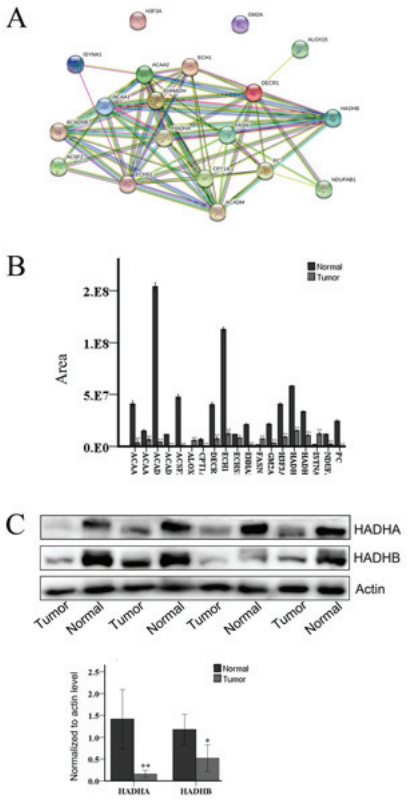

Figure 4. STRING analysis shows the interactions of the 19 lipid metabolism-related proteins. (A) Visualization of protein-protein interactions of the proteins in Wilms' tumors using STRING analysis (confidence mode) revealed the associations among the 19 proteins. Lines represent interactions between proteins. (B) Statistical data of the expression of the 19 lipid metabolism-related protein. (C) Western blotting of hydroxyacyl coenzyme A dehydrogenase (HADH)A and HADHB revealed marked interaction with fatty acid synthase expression in Wilms' tumor and its adjacent tissue (*P<0.05 and **P<0.01). Actin was used as a loading control.

acid degradation (the EC code is used in the figure instead of the related enzyme). It was observed that the HADH, HAHDB, ACAA1 and ACAA2 proteins all hold important positions in the KEGG signaling pathway and participate in this process.

Quantitative informatics analysis of IPA. IPA analysis revealed that protein metabolism in Wilms' tumors is closely associated with tumor cell death, cell cycle, and lipid metabolism (Fig. 5). Lipid metabolism plays an important role in tumors, and signaling pathway analysis has demonstrated that dysregulated proteins play an important role in fatty acid metabolism and are involved in the classical pathways, apoptosis and autophagy of multiple tumors (Fig. 5). Signaling pathway analysis revealed that dysregulated proteins play an important role in fatty acid metabolism pathways, and that sirtuin plays a key role in multiple tumors (Fig. 6). It may be inferred from the regulatory sub-effector network that FASN is involved in cell migration, cell proliferation and tumor necrosis at important positions in the total regulatory network and is implicated in various signaling pathways (Fig. 7).

Validation of FASN expression between Wilms' tumor and adjacent tissues. Next, MS was used to determine whether the expression of FASN in tumors was higher compared with that in adjacent tissues (Fig. 2). Analysis of the Oncomine

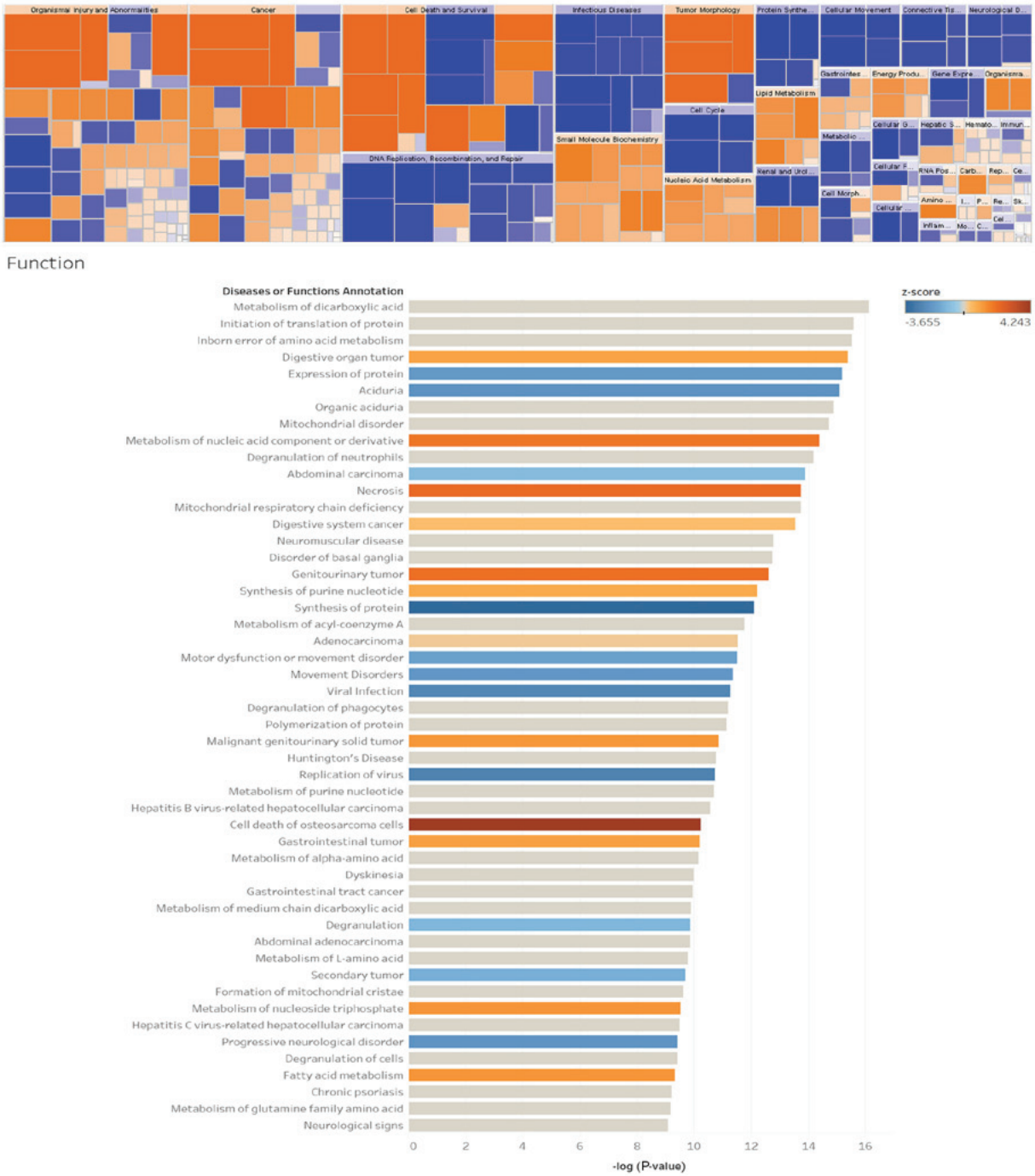

Figure 5. IPA of 437 dysregulated proteins in Wilms' tumor and adjacent normal tissues. IPA can replace the z-score of each major class and its subclasses with orange and blue, and the P-value is replaced by the block size for clustering. IPA, Ingenuity Pathway Analysis.

database, RT-qPCR, immunohistochemistry, western blotting and immunofluorescence were further performed to verify the results (Figs. 8 and 9). Oncomine database analysis demonstrated that FASN gene expression was significantly increased in Wilms' tumors (P=0.005 vs. normal tissue; Fig. 8A). Then, RT-PCR was used to detect the expression of FASN in 20 pairs of tumors and adjacent tissues, and the expression of FASN was found to be upregulated in Wilms' tumors (P<0.01; Fig. 8B). The results of immunohistochemistry, western blotting and immunofluorescence all verified that the expression of the FASN protein was significantly increased in tumors compared with that in adjacent tissues.

FASN expression and its correlation with clinicopathological parameters. The protein expression of FASN and the clinicopathological parameters of the patients are summarized in Table I. Among Wilms' tumor tissues, positive staining signals of FASN were detected in 34 samples (52.31%) with high immunoreactivity and 31 (47.69%) with low immunoreactivity. The association between FASN expression and tumor stage (III vs. I, P=0.001; II vs. I, P=0.007) and histopathological type (P=0.032) was statistically significant. There was no significant correlation between FASN expression and patient sex or age (P=0.620 and P=0.083, respectively).

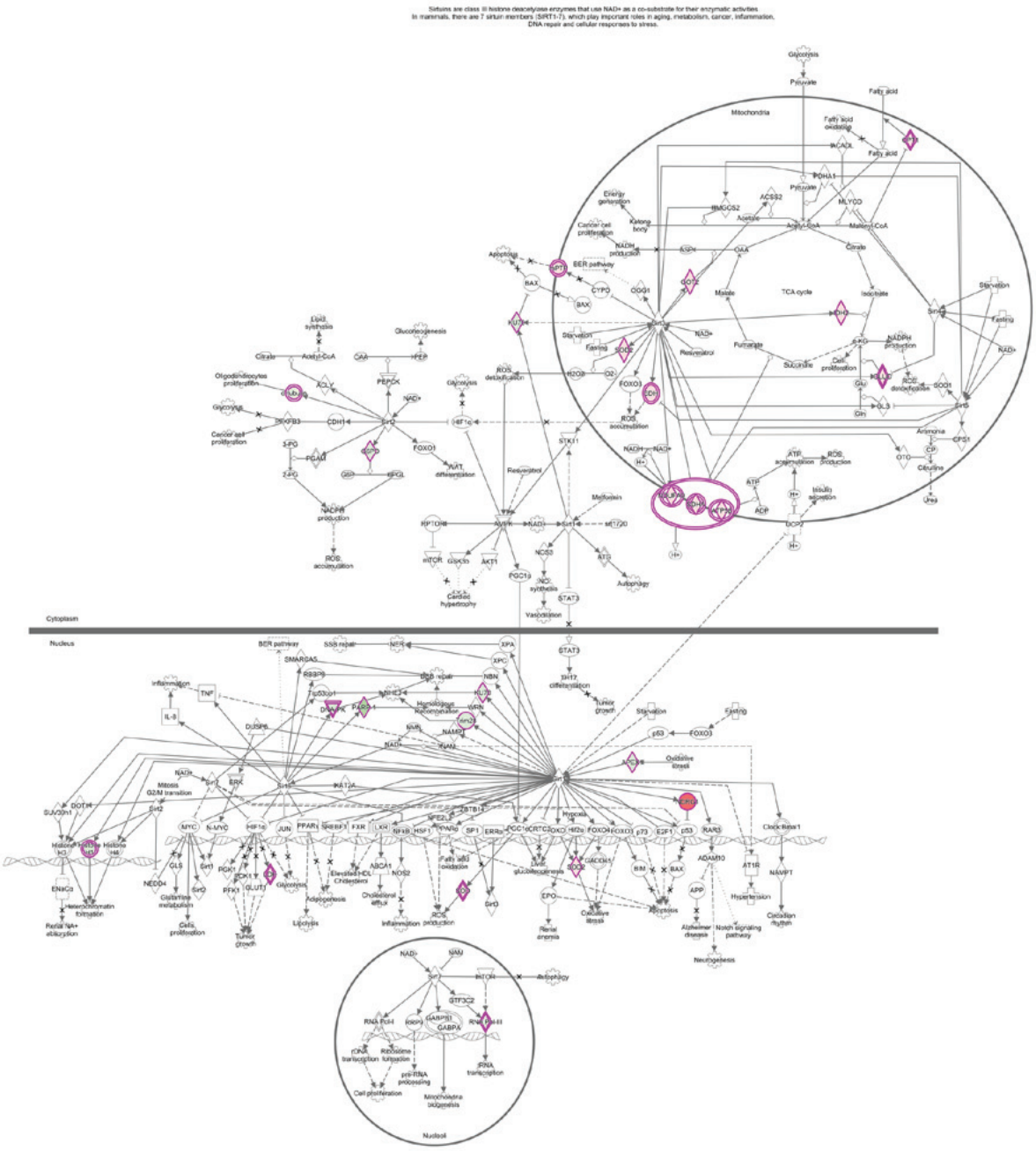

Figure 6. Post-translational modification involved in the regulation of dysregulated proteins by IPA. IPA scientists have manually mapped >800 biological signaling pathways and metabolic pathways, scoring the most relevant dysregulation pathways with experimental data in canonical pathways analysis. The Overlay and Path Designer tools personalize the editing and extension of the path. In addition, IPA's unique z-score algorithm also covers the analysis of activation inhibition regulation of nearly 200 pathways to quickly identify relevant pathways with obvious imbalances. Sirtuin (NAD-dependent deacetylase) is involved in the process of protein deacetylation, which includes important processes, such as fatty acid metabolism. IPA, Ingenuity Pathway Analysis.

Survival analysis. Postoperative follow-up was performed for the 65 Wilms' tumor patients (Fig. 10). In the univariate analysis, the Kaplan-Meier survival curves demonstrated that the survival of patients with high FASN expression was significantly shorter compared with that of patients with low FASN expression (P=0.016).

Discussion

Wilms' tumor is the most common pediatric malignant tumor of the urinary system, and its incidence rate is ~1/10,000 (20). As the tumor site is concealed, the tumor is usually diagnosed at an advanced stage, and there are currently no specific tumor markers. Wilms' tumor poses a serious threat to the patients' wellbeing and the search for novel anticancer targets to improve the clinical efficacy of Wilms' tumor treatment has been attracting increasing attention.

Lipid metabolism is an important and complex biochemical reaction in the body involving numerous enzymes. This process entails the digestion, absorption, synthesis and decomposition of fat in living organisms. Fat is processed into the substances required by the body to ensure the operation of normal physiological functions (21). Lipids are important substances that serve as energy storage and energy supply, and

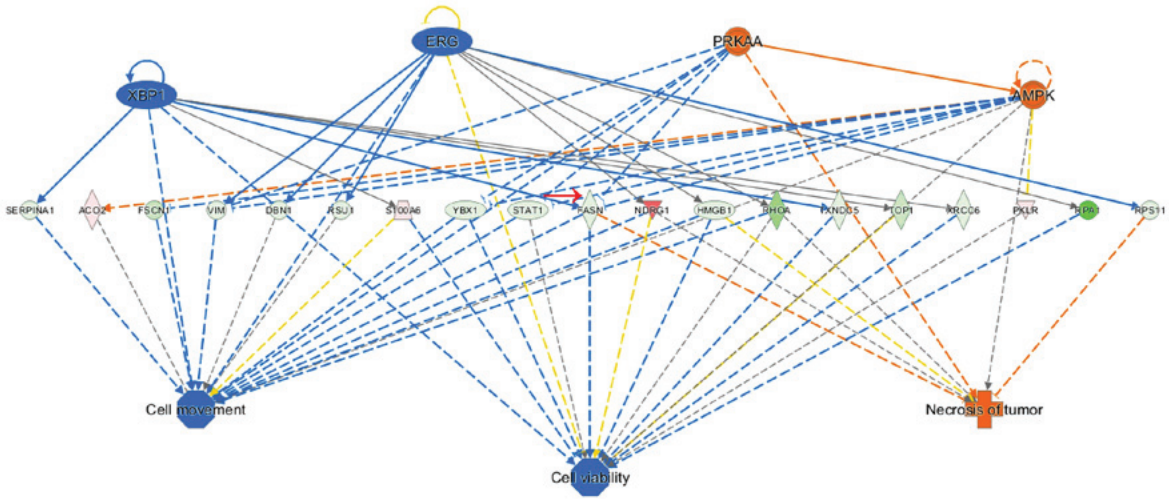

Figure 7. IPA further clusters the biological functions that may be exerted by each sub-network of transcriptional regulators to find a common regulatory-function network. The important role of FASN in the overall regulatory network is through its involvement in processes including cell migration, cell proliferation and tumor necrosis, and its association with a variety of signaling pathways. IPA, Ingenuity Pathway Analysis; FASN, fatty acid synthase.

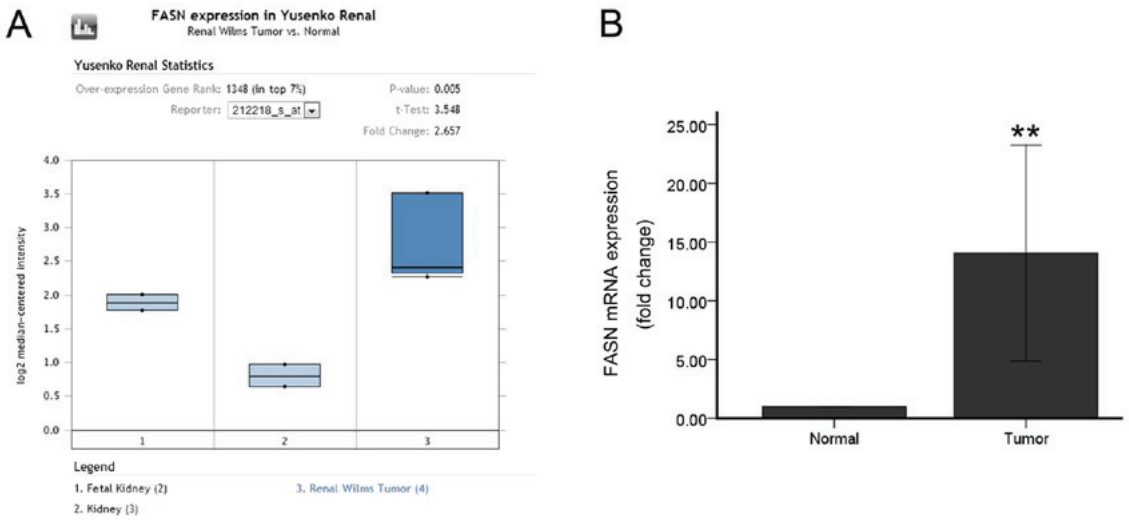

Figure 8. Oncomine database and RT-qPCR analyses were used to verify the expression of FASN at the gene level. (A) According to the Oncomine database, FASN gene expression was significantly increased in Wilms' tumors (P=0.005 vs. normal tissue). (B) RT-PCR was used to examine FASN expression in 20 pairs of tissues, including 10 Wilms' tumors and respective adjacent tissues. FASN gene expression was found to be upregulated in tumor tissues (**P<0.01 vs. adjacent tissue). Data are expressed as the mean ± standard deviation of 3 independent experiments. FASN, fatty acid synthase; RT, reverse transcription; qPCR, quantitative polymerase chain reaction.

phospholipids are important structural components of biofilms. Currently, due to the high metabolic properties of tumors, the study of energy metabolism in tumors has been attracting increasing attention from researchers, as is the interrelationship between lipid metabolism and the tumor. Lipid metabolism is closely associated with the proliferation, invasion, migration, radiosensitivity and chemosensitivity of various tumors, such as lobular lung, breast and prostate cancer (6,22,23). As regards the energy metabolism of Wilms' tumors, current research mainly focuses on glucose metabolism, whereas lipid metabolism has been less extensively studied. In our experiments, preliminary screening was performed by MS of tumor and adjacent tissues. Among the 437 proteins identified, 19 lipid metabolism-related proteins were differentially expressed. When these 19 lipid metabolism proteins were analyzed using KEGG, 11 proteins were found to be involved in the process of long chain elongation and degradation of fatty acids. Certain proteins exhibited synergy, such as EHHADH and HAHDA, which are involved in the conversion of (S)-3-hydroxy-dodecanoyl-CoA to 3-oxo-decanoyl-CoA. The 19 differentially expressed proteins were further analyzed: A total of 16 proteins exhibited low expression (HADHB, ACAA1, ACAA2, CPT1A, ECHS1, ACSF2, EHHADH, PC, ACADM, ACADSB, ECH1, GM2A, DECR1, HADHA, NDUFAB1 and H3F3A), and 3 proteins (FASN, ISYNA1 and ALOX15) were highly expressed. In addition, these 16 proteins and ALOX15 are associated with the metabolism of lipids. FASN and ISYNA1 are involved in the process of lipid synthesis. To a certain extent, lipid synthesis is active and degradation is inhibited in Wilms' tumors. The reason for this finding may be that the majority of the tissues we selected were from children who had not undergone chemoradiotherapy and

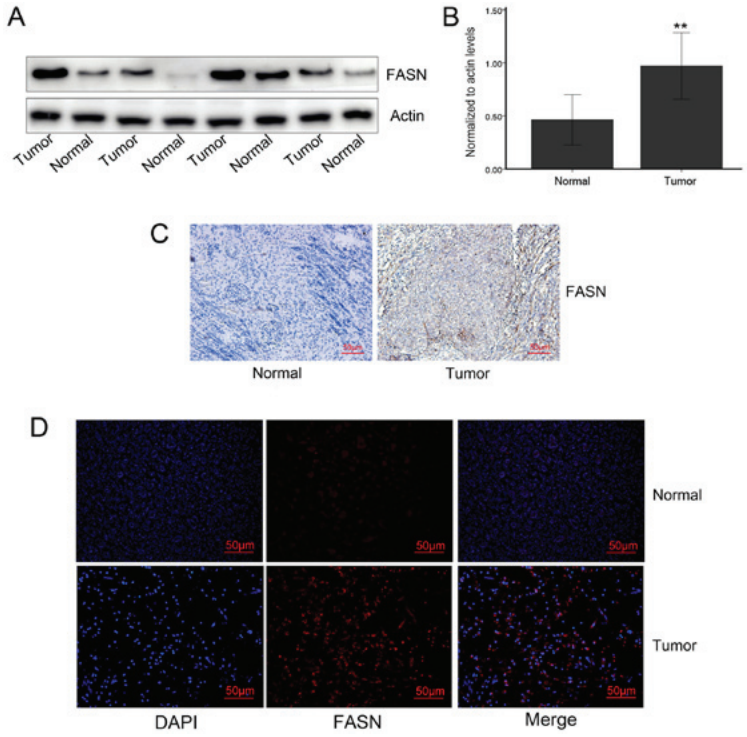

Figure 9. Molecular biology experiments were performed to verify the protein expression of FASN. (A) Western blotting of FASN expression in Wilms' tumor and its adjacent tissue. Actin was used as a loading control. (B) Quantification was performed by densitometric analysis and normalized to actin levels. **P<0.01 vs. adjacent tissue. Data are expressed as the mean ± standard deviation of 3 independent experiments. (C) Immunohistochemistry of FASN expression in Wilms' tumor and adjacent tissues. (D) Immunofluorescence of FASN expression in Wilms' tumor and adjacent tissues. FASN, fatty acid synthase.

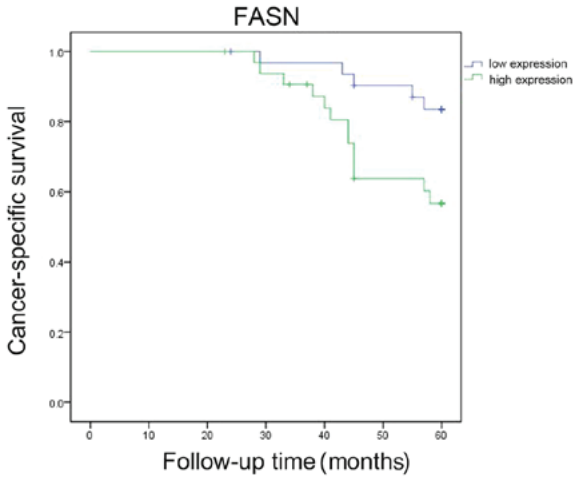

Figure 10. Survival curve analysis of the association between FASN and prognosis. The survival curves were analyzed by the Kaplan-Meier method. The follow-up time was 60 months. High expression of FASN indicated poor prognosis in Wilms' tumor patients (P=0.016 vs. low expression). FASN, fatty acid synthase.

the tumor was not under hypoxic conditions. Excessive glucose metabolism (24) may inhibit lipid degradation to a certain extent. However, phospholipids are the main constituents of cell membranes, and the proliferation of tumors is a highly active process that requires the support of lipid synthesis, which may explain the overexpression of synthetase.

IPA is an integrated biological pathway analysis software based on cloud computing. IPA analysis includes function, disease correlation analysis, biological downstream effect analysis, classical pathway correlation analysis, and pathway activity effect prediction (25,26). Through IPA analysis, the dysregulated proteins screened by MS were found to be mainly involved in biological processes, such as cell death, cell cycle progression and lipid metabolism. Although the level of lipid metabolism is relatively lower in tumors compared with that in the adjacent tissues, lipid metabolism plays an important role in tumors; signaling pathway analysis demonstrated that dysregulated proteins play an important role in fatty acid metabolic pathways in multiple tumors. The classical pathway is involved in tumor apoptosis and autophagy, and the dysregulated protein is implicated in the process of post-translational modification. Sirtuin (NAD-dependent deacetylase) plays a key role in the epigenetic regulation of gene expression by altering chromatin structure. This protein has been reported to deacetylate histones and non-histones. It has been demonstrated that sirtuin deacetylation of histones induces chromatin condensation, whereas acetylation of histone acetyltransferase leads to chromatin decondensation. This balance is crucial for maintaining normal cellular function, and any disruption in this process may lead to tumorigenesis (27). Sirtuin-mediated protein deacetylation has been considered to play an important role in cancer (28), and there are reports of dylinin expression disorders in a variety of human malignancies (29-31). IPA results revealed that sirtuin may be dysregulated in Wilms' tumors, and the fatty acid metabolism pathway may affect biological behaviors, such as proliferation, apoptosis and autophagy of Wilms' tumors by sirtuin. In addition, the dysregulated proteins can be identified from the regulatory sub-effector network: FASN, one of the lipid synthesis-related enzymes among the dysregulated proteins, holds an important

position in the total regulatory network and is involved in processes such as cell migration, cell proliferation and tumor necrosis. In addition, FASN is associated with a variety of signaling pathways.

Several other metabolic proteins in Wilms' tumors have been found to be reduced compared with their levels in normal tissues, such as aldehyde dehydrogenase and proteins associated with propionic acid and butyrate metabolism and long-chain fatty acid metabolism (24). FASN is a multi-enzyme protein that catalyzes fatty acid synthesis. This protein is not a single enzyme but a whole enzymatic system composed of two identical 272-kDa multifunctional polypeptides (32,33). Accumulating evidence shows that FASN expression is upregulated in various human cancers and confers a survival advantage to these cancer cells (12,34-36). FASN overexpression has also been associated with resistance to anticancer treatments, and FASN has been found to be closely associated with the prognosis of a variety of tumors (37,38); however, its role in Wilms' tumors has not been extensively investigated. The present study revealed high expression of FASN by MS screening. This finding was further verified by Oncomine database, RT-qPCR, western blot, immunofluorescence and immunohistochemistry analyses, which confirmed the high expression of FASN in Wilms' tumors. Furthermore, the clinical case parameters of 65 children with Wilms' tumors were analyzed and it was observed that the expression of FASN was closely associated with tumor stage and pathological type, which confirmed that FASN may be implicated in the malignant progression of Wilms' tumors. In addition, the results of the survival analysis revealed that the prognosis of patients with high expression of FASN was relatively poor, which may be used as a biomarker to predict the prognosis. Therefore, the findings of the present study may provide a theoretical basis for subsequent experiments *in vivo* and *in vitro*, and help identify new targets for the treatment of Wilms' tumors.

Reprogramming cellular energy metabolism is one of the major markers of cancer, and cancer cells rely on fatty acids as a building block for cell proliferation; thus, disrupting key enzymes or modulators in cellular metabolism may be a promising new approach to cancer therapy (39,40). Targeting lipid metabolism has provided novel ideas for the treatment of tumors (24). In particular, there is an increasing number of studies on targeted therapies for FASN, and inhibition of FASN expression may be of therapeutic value in a variety of tumors. In addition to the specific inhibitors of FASN, such as C75, Fasnall, and EGCG (41-43), which may exert antitumor effects, researchers committed to design specific drugs for FASN and discovered a new antitumor drug, 'compound 34' for treating various tumors (44). Other studies have also sought to treat tumors by identifying upstream regulators of FASN or miRNAs (7,45). In other tumors, the study of FASN is not limited to clinical specimens; through cell and animal experiments, its mechanism of action has been investigated and was found to include the AKT/mTOR signaling pathway, which is closely associated with tumors (46,47). To a certain extent, these previous studies may explain the effectiveness of targeting FASN for tumor treatment. In addition, the present study may also be of value as a guide for the treatment of Wilms' tumors, for which the targeted inhibition of FASN may prove useful.

Although extensive studies on cancer and its initiation are beginning to unravel the role of lipid metabolism in this process, the lipid metabolism-related enzymes that are implicated in Wilms' tumor have not been determined. Due to the low incidence of pediatric vs. adult tumors, there were relatively few cases included in the present study. However, the abovementioned MS screening may provide novel ideas for the study of lipid metabolism in Wilms' tumors, which may serve as a reference for subsequent research. In addition, FASN appeared to be a useful biomarker for Wilms' tumors based on the analysis of the prognosis of 65 pediatric patients. This index provides theoretical support for the prognosis assessment of children with Wilms' tumors. Moreover, FASN may prove to be useful in the targeted therapy of Wilms' tumor.

Acknowledgements

Not applicable.

Funding

The present study was supported by funding provided by the National Natural Science Foundation (grant no. 81400575), the Hunan Provincial Natural Science Foundation of China (grant no. 2017JJ4071), the Science and Technology Development Plan Project of Shandong Province, China (grant nos. 2014GSF118144, 2018GSF118209 and 2019GSF108061), Jinan Science and Technology Bureau (grant no. 201602170) and the Shandong Provincial Natural Science Foundation (grant nos. ZR2017MH091 and ZR2015HM048).

Availability of data and materials

The datasets used and/or analyzed during the present study are available from the corresponding author on reasonable request.

Authors' contributions

XQW and GQD conceived and designed the study. XQW, YDW and YFZ contributed to the work by designing and performing the experiments, collecting and analyzing data, and drafting the manuscript. FG collected patient samples and conceived the experiments. WL and RDW read and approved the final manuscript.

Ethics approval and consent to participate

The study was approved by the Ethics Committee of the Provincial Hospital affiliated to Shandong University (approval no. 2019-124). All the included specimens were obtained following informed consent by the patients' guardians, and the patient data were anonymized. The research protocol conformed to the principles outlined in the Declaration of Helsinki.

Patient consent for publication

Not applicable.

Competing interests

All the authors declare that they have no competing interests.

References

1. Jiang C, Li X, Zhao H and Liu H: Long non-coding RNAs: Potential new biomarkers for predicting tumor invasion and metastasis. Mol Cancer 15: 62, 2016.
2. Long J, Zhang CJ, Zhu N, Du K, Yin YF, Tan X, Liao DF and Qin L: Lipid metabolism and carcinogenesis, cancer development. Am J Cancer Res 8: 778-791, 2018.
3. Gómez de Cedrón M and Ramírez de Molina A: Microtargeting cancer metabolism: Opening new therapeutic windows based on lipid metabolism. J Lipid Res 57: 193-206, 2016.
4. Huang C and Freter C: Lipid metabolism, apoptosis and cancer therapy. Int J Mol Sci 16: 924-949, 2015.
5. Luo X, Cheng C, Tan Z, Li N, Tang M, Yang L and Cao Y: Emerging roles of lipid metabolism in cancer metastasis. Mol Cancer 16: 76, 2017.
6. Deep G and Schlaepfer IR: Aberrant Lipid Metabolism Promotes Prostate Cancer: Role in Cell Survival under Hypoxia and Extracellular Vesicles Biogenesis. Int J Mol Sci 17: 17, 2016.
7. Duan J, Chen L, Zhou M, Zhang J, Sun L, Huang N, Bin J, Liao Y and Liao W: MACC1 decreases the chemosensitivity of gastric cancer cells to oxaliplatin by regulating FASN expression. Oncol Rep 37: 2583-2592, 2017.
8. Smith S, Witkowski A and Joshi AK: Structural and functional organization of the animal fatty acid synthase. Prog Lipid Res 42: 289-317, 2003.
9. Szolkiewicz M, Nieweglowski T, Korczynska J, Sucajtys E, Stelmanska E, Goyke E, Swierczynski J and Rutkowski B: Upregulation of fatty acid synthase gene expression in experimental chronic renal failure. Metabolism 51: 1605-1610, 2002.
10. Liu H, Liu JY, Wu X and Zhang JT: Biochemistry, molecular biology, and pharmacology of fatty acid synthase, an emerging therapeutic target and diagnosis/prognosis marker. Int J Biochem Mol Biol 1: 69-89, 2010.
11. Heuer TS, Ventura R, Mordec K, Lai J, Fridlib M, Buckley D and Kemble G: FASN Inhibition and Taxane Treatment Combine to Enhance Anti-tumor Efficacy in Diverse Xenograft Tumor Models through Disruption of Tubulin Palmitoylation and Microtubule Organization and FASN Inhibition-Mediated Effects on Oncogenic Signaling and Gene Expression. EBioMedicine 16: 51-62, 2017.
12. Papaevangelou E, Almeida GS, Box C, deSouza NM and Chung YL: The effect of FASN inhibition on the growth and metabolism of a cisplatin-resistant ovarian carcinoma model. Int J Cancer 143: 992-1002, 2018.
13. Ventura R, Mordec K, Waszczuk J, Wang Z, Lai J, Fridlib M, Buckley D, Kemble G and Heuer TS: Inhibition of de novo Palmitate Synthesis by Fatty Acid Synthase Induces Apoptosis in Tumor Cells by Remodeling Cell Membranes, Inhibiting Signaling Pathways, and Reprogramming Gene Expression. EBioMedicine 2: 808-824, 2015.
14. Albiges L, Hakimi AA, Xie W, McKay RR, Simantov R, Lin X, Lee JL, Rini BI, Srinivas S, Bjarnason GA, *et al*: Body Mass Index and Metastatic Renal Cell Carcinoma: Clinical and Biological Correlations. J Clin Oncol 34: 3655-3663, 2016.
15. Camassei FD, Jenkner A, Ravà L, Bosman C, Francalanci P, Donfrancesco A, Alò PL and Boldrini R: Expression of the lipogenic enzyme fatty acid synthase (FAS) as a predictor of poor outcome in nephroblastoma: An interinstitutional study. Med Pediatr Oncol 40: 302-308, 2003.
16. Fuhrman SA, Lasky LC and Limas C: Prognostic significance of morphologic parameters in renal cell carcinoma. Am J Surg Pathol 6: 655-663, 1982.
17. Nagaprashantha LD, Talamantes T, Singhal J, Guo J, Vatsyayan R, Rauniyar N, Awasthi S, Singhal SS and Prokai L: Proteomic analysis of signaling network regulation in renal cell carcinomas with differential hypoxia-inducible factor-2α expression. PLoS One 8: e71654, 2013.
18. Wang Q, Geng F, Zhou H, Chen Y, Du J, Zhang X, Song D and Zhao H: MDIG promotes cisplatin resistance of lung adenocarcinoma by regulating ABC transporter expression via activation of the WNT/β-catenin signaling pathway. Oncol Lett 18: 4294-4307, 2019.
19. Livak KJ and Schmittgen TD: Analysis of relative gene expression data using real-time quantitative PCR and the 2(-Delta Delta C(T)) Method. Methods 25: 402-408, 2001.
20. Friedman AD: Wilms tumor. Pediatr Rev 34: 328-330, discussion 330, 2013.
21. Werbrouck E, Van Gansbeke D, Vanreusel A and De Troch M: Temperature Affects the Use of Storage Fatty Acids as Energy Source in a Benthic Copepod (*Platychelipus littoralis*, Harpacticoida). PLoS One 11: e0151779, 2016.
22. Cha YJ, Kim HM and Koo JS: Expression of Lipid Metabolism-Related Proteins Differs between Invasive Lobular Carcinoma and Invasive Ductal Carcinoma. Int J Mol Sci 18: 18, 2017.
23. Kim S, Lee Y and Koo JS: Differential expression of lipid metabolism-related proteins in different breast cancer subtypes. PLoS One 10: e0119473, 2015.
24. Aminzadeh S, Vidali S, Sperl W, Kofler B and Feichtinger RG: Energy metabolism in neuroblastoma and Wilms tumor. Transl Pediatr 4: 20-32, 2015.
25. Liu X, Wen F, Yang J, Chen L and Wei YQ: A review of current applications of mass spectrometry for neuroproteomics in epilepsy. Mass Spectrom Rev 29: 197-246, 2010.
26. Thomas S and Bonchev D: A survey of current software for network analysis in molecular biology. Hum Genomics 4: 353-360, 2010.
27. Glozak MA, Sengupta N, Zhang X and Seto E: Acetylation and deacetylation of non-histone proteins. Gene 363: 15-23, 2005.
28. Glozak MA and Seto E: Histone deacetylases and cancer. Oncogene 26: 5420-5432, 2007.
29. Chen X, Sun K, Jiao S, Cai N, Zhao X, Zou H, Xie Y, Wang Z, Zhong M and Wei L: High levels of SIRT1 expression enhance tumorigenesis and associate with a poor prognosis of colorectal carcinoma patients. Sci Rep 4: 7481, 2014.
30. Hao C, Zhu PX, Yang X, Han ZP, Jiang JH, Zong C, Zhang XG, Liu WT, Zhao QD, Fan TT, *et al*: Overexpression of SIRT1 promotes metastasis through epithelial-mesenchymal transition in hepatocellular carcinoma. BMC Cancer 14: 978, 2014.
31. Wang RH, Sengupta K, Li C, Kim HS, Cao L, Xiao C, Kim S, Xu X, Zheng Y, Chilton B, *et al*: Impaired DNA damage response, genome instability, and tumorigenesis in SIRT1 mutant mice. Cancer Cell 14: 312-323, 2008.
32. Alberts AW, Strauss AW, Hennessy S and Vagelos PR: Regulation of synthesis of hepatic fatty acid synthetase: Binding of fatty acid synthetase antibodies to polysomes. Proc Natl Acad Sci USA 72: 3956-3960, 1975.
33. Stoops JK, Arslanian MJ, Oh YH, Aune KC, Vanaman TC and Wakil SJ: Presence of two polypeptide chains comprising fatty acid synthetase. Proc Natl Acad Sci USA 72: 1940-1944, 1975.
34. Jiang Y, Yin X, Wu L, Qin Q and Xu J: MAPK/P53-mediated FASN expression in bone tumors. Oncol Lett 13: 4035-4038, 2017.
35. O'Malley J, Kumar R, Kuzmin AN, Pliss A, Yadav N, Balachandar S, Wang J, Attwood K, Prasad PN and Chandra D: Lipid quantification by Raman microspectroscopy as a potential biomarker in prostate cancer. Cancer Lett 397: 52-60, 2017.
36. Patel AV, Johansson G, Colbert MC, Dasgupta B and Ratner N: Fatty acid synthase is a metabolic oncogene targetable in malignant peripheral nerve sheath tumors. Neuro-oncol 17: 1599-1608, 2015.
37. Diaz KP, Gondak R, Martins LL, de Almeida OP, León JE, Mariano FV, Altemani A and Vargas PA: Fatty acid synthase and Ki-67 immunoexpression can be useful for the identification of malignant component in carcinoma ex-pleomorphic adenoma. J Oral Pathol Med 48: 232-238, 2019.
38. Sangeetha M, Deepa PR, Rishi P, Khetan V and Krishnakumar S: Global gene deregulations in FASN silenced retinoblastoma cancer cells: Molecular and clinico-pathological correlations. J Cell Biochem 116: 2676-2694, 2015.
39. Currie E, Schulze A, Zechner R, Walther TC and Farese RV Jr: Cellular fatty acid metabolism and cancer. Cell Metab 18: 153-161, 2013.
40. Ooi AT and Gomperts BN: Molecular Pathways: Targeting Cellular Energy Metabolism in Cancer via Inhibition of SLC2A1 and LDHA. Clin Cancer Res 21: 2440-2444, 2015.
41. Alwarawrah Y, Hughes P, Loiselle D, Carlson DA, Darr DB, Jordan JL, Xiong J, Hunter LM, Dubois LG, Thompson JW, *et al*: Fasnall, a Selective FASN Inhibitor, Shows Potent Anti-tumor Activity in the MMTV-Neu Model of HER2(+) Breast Cancer. Cell Chem Biol 23: 678-688, 2016.

42. Wong A, Chen S, Yang LK, Kanagasundaram Y and Crasta K: Lipid accumulation facilitates mitotic slippage-induced adaptation to anti-mitotic drug treatment. Cell Death Discov 4: 109, 2018.
43. Giro-Perafita A, Palomeras S, Lum DH, Blancafort A, Viñas G, Oliveras G, Pérez-Bueno F, Sarrats A, Welm AL and Puig T: Preclinical Evaluation of Fatty Acid Synthase and EGFR Inhibition in Triple-Negative Breast Cancer. Clin Cancer Res 22: 4687-4697, 2016.
44. Lu T, Schubert C, Cummings MD, Bignan G, Connolly PJ, Smans K, Ludovici D, Parker MH, Meyer C, Rocaboy C, *et al*: Design and synthesis of a series of bioavailable fatty acid synthase (FASN) KR domain inhibitors for cancer therapy. Bioorg Med Chem Lett 28: 2159-2164, 2018.
45. Singh R, Yadav V, Kumar S and Saini N: MicroRNA-195 inhibits proliferation, invasion and metastasis in breast cancer cells by targeting FASN, HMGCR, ACACA and CYP27B1. Sci Rep 5: 17454, 2015.
46. Shen M, Tsai Y, Zhu R, Keng PC, Chen Y, Chen Y and Lee SO: FASN-TGF-β1-PD-L1 axis contributes to the development of resistance to NK cell cytotoxicity of cisplatin-resistant lung cancer cells. Biochim Biophys Acta Mol Cell Biol Lipids 1863: 313-322, 2018.
47. Tao T, Su Q, Xu S, Deng J, Zhou S, Zhuang Y, Huang Y, He C, He S, Peng M, *et al*: Down-regulation of PKM2 decreases FASN expression in bladder cancer cells through AKT/mTOR/SREBP-1c axis. J Cell Physiol 234: 3088-3104, 2019.